Journal of Environmental Chemical Engineering 14 (2026) 124661

Contents lists available at ScienceDirect

Journal of Environmental Chemical Engineering

journal homepage: www.elsevier.com/locate/jece

Cobalt recovery from lithium cobalt oxide cathode scraps via green solvents: Process development and life cycle assessment

Shoayb Mojtahedi [a,b,1], Leonardo Sparascio [c,1], Federico Mascetti [a], Salan Xierzati [a], Andrea Vitale [a], Simone D'Agostino [a], Chiara Samorì [a], Alessandro Girolamo Rombolà [a], Nicolas Greggio [a], Daniele Cespi [c,d,*], Fabrizio Passarini [c,d], Chiara Zentile [c], Antunes Staffolani [a,b], Ncholu Manyala [e], Francesca Soavi [a,b]

[a] Department of Chemistry "Giacomo Ciamician", Alma Mater Studiorum University of Bologna, Via Gobetti 85, Bologna 40129, Italy
[b] ENERCube Lab, Centro Ricerche Energia, Ambiente e Mare, Centro Interdipartimentale per la Ricerca Industriale Fonti Rinnovabili, Ambiente, Mare ed Energia (CIRI-FRAME) – Alma Mater Studiorum University of Bologna, Viale Ciro Menotti, 48, Marina di Ravenna 48122, Italy
[c] Department of Industrial Chemistry "Toso Montanari", Alma Mater Studiorum University of Bologna, Via Gobetti 85, Bologna 40129, Italy
[d] Interdepartmental Centre for Industrial Research – Renewable Resources, Environment, Sea and Energy, University of Bologna, Via D. Campana 71, Rimini 47923, Italy
[e] Department of Physics, University of Pretoria, Pretoria, South Africa

ARTICLE INFO

Keywords:
Lithium-ion battery cathode recycling
Cobalt
Deep eutectic solvent
Triethyl phosphate
LCA

ABSTRACT

A recycling process for recovering cobalt from lithium-ion battery cathode production scraps is investigated using green solvents. The method combines electrode delamination with triethyl phosphate (TEP), dissolution of the recovered active material in a deep eutectic solvent (DES) composed of choline chloride and oxalic acid (1:1 molar ratio), and selective cobalt precipitation via controlled pH adjustment with KOH. The recovered black mass was characterized by Powder X-ray diffraction PXRD and Thermogravimetric analysis (TGA), confirming structural integrity of $LiCoO_2$ after TEP treatment and a purity of ~98.25%. Following DES leaching and precipitation at pH 12, a highly crystalline mixed cobalt oxide/hydroxide phase (CoO_2/$Co(OH)_2$) was obtained with a purity of 99.12%. Microwave Plasma Atomic Emission Spectroscopy (MP-AES) analysis verified effective cobalt–lithium separation, with cobalt exclusively recovered in the solid phase. A cobalt recovery efficiency of 57% was achieved at lab scale, with losses primarily attributed to material handling at low Technology Readiness Level (TRL) rather than process inefficiency. A cradle-to-gate Life Cycle Assessment (LCA) was conducted using primary experimental inventory data. Environmental hotspot analysis identified DES preparation and the leaching step as the dominant contributors across most impact categories, driven respectively by solvent production (oxalic acid and choline chloride) and electricity consumption. Sensitivity and uncertainty analyses confirmed model robustness and highlighted renewable energy transition and solvent optimization as key levers for future improvement. This early-stage LCA provides a quantitative environmental baseline to support eco-design and scale-up of DES-based cobalt recovery from lithium cobalt oxide (LCO) cathode waste.

1. Introduction

Lithium-ion batteries (LIBs) have become indispensable in modern energy storage systems, powering consumer electronics, electric vehicles, and renewable energy stationary storage [1–3]. LIB performance, energy density, and lifespan are largely determined by the composition and quality of the cathode materials, which include lithium cobalt oxide (LCO), lithium nickel manganese cobalt oxide (NMC), lithium iron phosphate (LFP), and lithium nickel cobalt aluminium oxide (NCA) [4–6]. Metals such as lithium, cobalt, nickel, and manganese are elements whose extraction and refining pose substantial environmental and socio-economic challenges and are, therefore, listed as Critical Raw Materials by Europe [7–10].

By recovering valuable metals such as lithium, cobalt, nickel, and

* Corresponding author at: Department of Industrial Chemistry "Toso Montanari", Alma Mater Studiorum University of Bologna, Via Gobetti 85, Bologna 40129, Italy.
E-mail address: daniele.cespi2@unibo.it (D. Cespi).
[1] Both authors contributed equally.

https://doi.org/10.1016/j.jece.2026.124661
Received 22 June 2026; Received in revised form 10 August 2026; Accepted 15 August 2026
Available online 16 August 2026

manganese from spent batteries, recycling reduces the demand for raw material extraction, mitigates environmental damage caused by mining, and decreases the strain on natural resources [11–13]. Furthermore, recycling processes can stabilize the supply chain, reducing risks related to the geopolitical and socio-economic challenges of sourcing from specific regions [14,15].

In addition to spent LIB electrodes, production scraps constitute a significant secondary source of critical raw materials. However, because these scraps do not directly contribute to the material supply for battery manufacturing, their generation effectively increases the demand for primary raw materials. Consequently, the systematic recovery of production scraps can play a crucial role in mitigating supply constraints and strengthening the overall resilience of critical raw material source within the LIB value chain [16].

Recycling methods for lithium-ion battery cathodes typically fall into three main categories: pyrometallurgical, hydrometallurgical, and direct recycling [17]. Pyrometallurgical recycling involves high-temperature smelting to extract metals from battery materials. However, this process is energy-intensive, emits greenhouse gases, and often results in the loss of lithium due to the high temperatures, leading to low overall recovery efficiency [18]. Hydrometallurgical recycling uses chemical leaching to dissolve metals from the battery materials, followed by selective precipitation or solvent extraction to recover individual metals. It allows for high recovery rates of lithium, cobalt, nickel, and manganese, often with greater purity than pyrometallurgical methods. Hydrometallurgical recycling is more environmentally friendly and energy-efficient, with lower temperatures required, but it involves the handling and disposal of potentially hazardous chemicals, which can create environmental challenges if not managed carefully [19]. In the Direct Recycling method, battery components are recovered and reconditioned with minimal chemical processing, allowing the cathode material to be directly reused in new batteries. This approach preserves the complex structures of the cathode material, potentially reducing the need for re-synthesis and conserving energy. The main advantage of direct recycling is that it can maintain the cathode's functional structure, saving energy and reducing chemical waste. However, it requires careful sorting and assessment of battery health, making it technically complex and not yet scalable for a wide range of battery chemistries [20].

Hence, each method has unique advantages and limitations, with pyrometallurgy favored for simplicity, hydrometallurgy for high recovery efficiency, and direct recycling for preserving cathode material structure [21]. The hydrometallurgical route is currently the most widely adopted method, primarily due to its ability to achieve high metal purity and recovery rates. This approach typically involves four main stages: i) pre-treatment of spent LIBs; ii) separation of the active material from the current collector; iii) leaching; and iv) recovery of valuable metals from the leachate material [17].

LIB electrodes are composed of active materials, carbon, and binder, the so-called black mass, cast on metal current collectors. The commonly used binder is poly (vinylidene difluoride) (PVdF), which conventionally needs N-methyl−2-pyrrolidone (NMP) as solvent, both very toxic for humans and the environment. Europe included NMP in the list of very high concern substances and set severe limits on its use. The presence of F-containing polymers generates volatile and toxic fluorocarbons during traditional incineration, as well as the LIBs' disposal might generate harmful substances and incombustible waste materials that need to be landfilled [22,23].

Physical separation of the black mass (BM) from the current collector is among the most effective options for pre-treating LIBs and isolating valuable components, offering both economic and environmental advantages. Organic solvents with strong affinity for the polymer binder such as N-Methyl−2-pyrrolidone (NMP), Dimethylacetamide (DMAC), Dimethylformamide (DMF), and Dimethyl Sulfoxide (DMSO), are commonly employed to weaken adhesion between the current collector and the active material, often under sonication. However, the waste solutions generated in this process pose environmental risks and therefore require proper treatment [24]. This has driven the development of greener alternatives. Citrus juices and, more recently, Cyrene, a bio-derived green solvent, have been proposed as environmentally friendly options, opening pathways toward more sustainable electrode separation and recovery processes [25,26]. Triethyl phosphate (TEP) is also emerging as a greener alternative to conventional organic solvents for PVdF dissolution and BM direct recovery [27].

Leaching is the central step of hydrometallurgy, where metals in cathode active materials are dissolved into ionic form, after which they can be recovered through chemical methods. Despite its effectiveness, hydrometallurgy is associated with significant environmental burdens due to the use of hazardous chemicals, long processing times, costly extractants, and the generation of secondary wastes such as acidic effluents, sludge, and high-salinity solutions, all of which must be managed appropriately [28].

Over the past two decades, deep eutectic solvents (DES) have emerged as promising candidates for addressing the environmental and economic challenges associated with LIB recycling [29]. DESs are a wide family of eutectic mixtures composed of neutral or ionic substances combined in specific molar ratios, which interact through hydrogen bonds and that deviate from the ideal thermodynamic behaviour [30]; in many formulations, DES components are low-cost, non-toxic and biodegradable [31,32].

Despite the growing body of literature on DES-based leaching of spent LIB cathodes, comprehensively reviewed by Chakrabarti et al., 2026 [33], two relevant gaps remain unaddressed. First, most studies focus on end-of-life battery black mass, whereas manufacturing scraps from LCO cathode production have received comparatively little attention as a feedstock for hydrometallurgical recovery. Second, while a limited number of works have coupled DES leaching with life cycle assessment (LCA), these have predominantly targeted NCM chemistries or non-LCO feedstocks, and have relied on secondary or simulated process data; as noted by Chakrabarti et al., 2026, robust process-level LCAs for DES-based battery recycling remain scarce and represent major research need [33–35]. In contrast, the present study investigates a targeted recycling strategy for real LCO cathode production scraps, combining TEP-assisted delamination for active material recovery with a choline chloride–oxalic acid DES-based leaching route for cobalt extraction. Furthermore, the environmental assessment is developed using primary experimental inventory data collected directly from laboratory-scale operations, including measured electricity consumption, rather than relying exclusively on literature-based or simulated datasets. This integrated experimental and environmental evaluation provides a more representative baseline for assessing the sustainability challenges and optimization opportunities of DES-based cobalt recovery processes at an early technology development stage. To the best of the authors' knowledge, no study has yet reported an integrated experimental and environmental assessment of DES-based cobalt recovery from LCO manufacturing scraps using primary laboratory-scale inventory data.

The present work addresses this gap by reporting both the optimisation of a DES leaching process for cobalt recovery from LCO cathode scraps and a cradle-to-gate LCA conducted on primary experimental data, with the aim of identifying environmental hotspots at an early stage of process development and providing a reference baseline for future scale-up assessments. Given the high solubility of transition metal oxides in many DESs [36], in this work, cobalt is recovered from LCO cathode scraps using a DES composed of choline chloride as the hydrogen bond acceptor and oxalic acid as the hydrogen bond donor. The recycling strategy includes electrode delamination with the green solvent TEP, dissolution of the recovered active material BM in the DES, and subsequent cobalt precipitation through controlled pH adjustment. An LCA study was then carried out to quantify the potential environmental impacts associated with the DES-enabled recovery of cobalt from primary LCO cathode scraps. Given the low Technology Readiness Level

(TRL) of the process, this assessment represents an early-stage LCA intended to identify the most impactful stages of the proposed recycling pathway and to inform subsequent optimization and eco-design for future scale-up.

Overall, while most previous studies have focused on recovering valuable metals from end-of-life LIB black mass through conventional hydrometallurgical or DES-based processes [37–39], the present work investigates real LCO cathode manufacturing scraps as an alternative and underexplored secondary resource focusing on an easy-to-be upscaled process performed at circum-ambient conditions by green solvents. Indeed, the proposed recycling strategy integrates green solvents of TEP-assisted electrode delamination with a choline chloride–oxalic acid DES leaching process. TEP enables the selective separation of the black mass from the aluminium current collector while preserving the structural integrity of the $LiCoO_2$ active material and simultaneously recovering the PVDF binder, thereby minimizing material degradation during the pretreatment stage [27]. Subsequently, cobalt is selectively recovered from the TEP-recovered black mass as crystalline mixed phase cobalt oxide/hydroxide through DES leaching followed by controlled pH precipitation. In addition to experimental process development, this study addresses a significant gap in literature by coupling the recycling route with a cradle-to-gate LCA analysis based entirely on primary laboratory-scale inventory data, including experimentally measured material and energy consumption. This integrated experimental and environmental assessment establishes a quantitative baseline for identifying environmental hotspots and guiding the eco-design and future scale-up of TEP/DES-based recycling processes for LCO production scraps. On the other word, the objective of this work was not to optimize the DES leaching parameters, but rather to evaluate the feasibility of integrating the TEP pretreatment with DES-based cobalt recovery and to perform a comprehensive environmental assessment of the overall recycling process.

2. Materials and methods

2.1. Reagents and materials

The cathode consisted of a lithium cobalt oxide electrode scrap shown in Fig. 1 (EV-ion resources 2003). Triethyl phosphate (TEP, purity ≥99%) and oxalic acid (≥99%) were purchased from Sigma-Aldrich; choline chloride (> 98%) was purchased from Thermo Scientific, and potassium hydroxide (KOH, Assay (acidimetric): ≥ 85.0%) was purchased from Merck. All the reagents were used without further purification.

2.2. Recycling process

Fig. 2 summarizes the processes that we have followed to recover Cobalt from the Electrode scraps. Each step is detailed in the following sections.

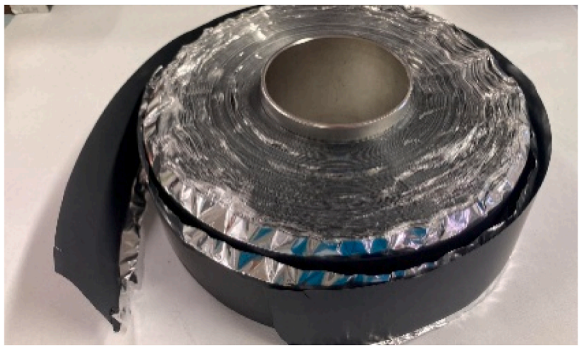

Fig. 1. The production roll scraps of the $LiCoO_2$ electrode.

2.2.1. Recovery of LCO BM from LCO electrode scraps via triethyl phosphate (TEP)

Physical separation of the BM from the current collector was performed by TEP treatment [27]. Specifically, several $LiCoO_2$ electrode pieces with an area of 1 cm^2 each were cut from the electrode roll and placed in the TEP for 1 h at 100 °C while stirring. The aluminium foils were separated from the solution by using a sieve. The resulting suspension was centrifuged at 6000 rpm for 10 min to separate the TEP solution containing carbon and binder. Afterwards, the collected precipitate was washed three times with water and dried at 60 °C in a thermostatic oven. The recovered BM was collected and labelled as LCO recovered.

2.2.2. BM leaching by DES and cobalt recovery

The DES was prepared by combining choline chloride (60.75 wt%) and oxalic acid (39.25 wt%), corresponding to a 1:1 molar ratio [40], followed by continuous stirring at 55 °C for 2 h [41]. The formation of the deep eutectic solvent was confirmed once the mixture became fully liquid, transparent, and homogeneous, thereby indicating complete hydrogen-bond interaction between the hydrogen bond acceptor (choline chloride) and the hydrogen bond donor (oxalic acid) component [41–43]. Afterwards, 1 g of the LCO recovered BM was added to the 40 g DES solution (solid to liquid ratio (S/L) 1:40 wt%) at 55°C while stirring for 48 h. The solution turned dark green. Finally, the resultant dark green suspension was centrifuged at 6000 rpm for 10 min to separate the undissolved part, and a green viscous liquid was formed. It was collected and placed in a beaker and the solution pH was progressively increased with the aim of precipitating cobalt oxide/hydroxide by adding small aliquots of KOH 5 M, while stirring at 50°C. The suspension was centrifuged at 6000 rpm for 10 min to separate the precipitate and solution after one hour of stirring. The brown precipitate was collected and dried at 80 °C overnight. The precipitate was filtered and washed with water to remove residues of oxalate species and ensure effective cobalt recovery.

2.3. Materials characterization

The thermogravimetric analysis (TGA) and Powder X-ray diffraction (PXRD) were conducted for the characterization of all recovered materials. TGA was performed under O_2 flow (60 mL/min) with a thermal ramp of 10 °C/min, using a TA Instruments Q50. PXRD measurements were carried out using a PANalytical Empyrean diffractometer equipped with a PIXcel3D detector and Cu Kα radiation (λ = 1.5418 Å, 40 kV, 40 mA). Data were recorded in Bragg–Brentano geometry over a 2θ range of 5–100° with a step size of 0.02626° and a counting time of 44.625 s per step. A 0.02 rad Soller slit was used on the diffracted beam side. Pulse Height Distribution (PHD) Levels range has been set between 45% and 80% to avoid Cobalt fluorescence due to X-Ray excitation.

Microwave plasma–atomic emission spectroscopy (MP-AES) was performed using an Agilent 4210 instrument (Agilent Technologies, USA) equipped with solvent-resistant tubing, a double-pass cyclonic spray chamber, and an inert flow-blurring nebulizer (OneNeb). Plasma generation was sustained with high-purity nitrogen supplied by an Agilent 4107 Nitrogen Generator (Agilent Technologies, CA, USA). Li and Co were quantified at 610.365 and 340.512 nm, respectively, selected for optimal signal-to-noise ratios and minimal spectral interferences. Ultrapure water blanks and two quality control standards (5 mg L^{-1} Li and Co in 2% (v/v) HNO_3) were analysed to monitor system cleanliness and carryover. Calibration standards were prepared from 1000 mg L^{-1} stock solutions obtained from Supelco (Li in 0.5 mol L^{-1} HNO_3) and VWR (Co in 2% HNO_3). Background correction was automatically applied using Agilent MP Expert software (Agilent Technologies, CA, USA). For MP-AES analyses, samples were prepared as follows. Approximately 0.2 g of each sample was weighed into a 100 mL glass beaker and treated with 20 mL of concentrated nitric acid (65% HNO_3). After a 20 min pre-digestion at room temperature, the beaker was

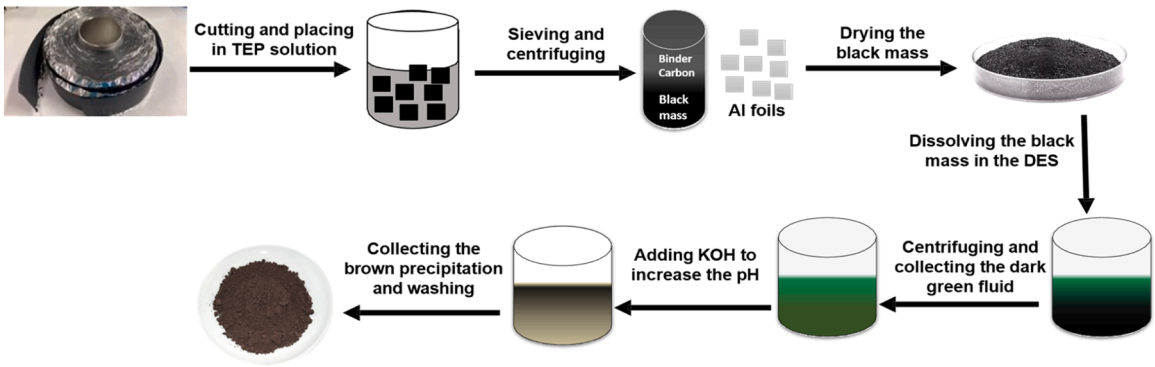

Fig. 2. Schematic of the cobalt recovery process.

covered with a watch glass and heated on a hot plate to gentle reflux. Digestion was carried out at 80 °C for 3 h, with additional HNO_3 added as needed to maintain reflux and prevent drying. After cooling to room temperature, the digest was filtered through ashless filter paper (Whatman, 150 mm × 100 mm) and diluted to the required volume with 5% (v/v) HNO_3 prior to MP-AES analysis.

2.4. LCA study

The LCA methodological framework, outlined in ISO 14040 and ISO 14044 standards, consists of four iterative phases [44,45]. The goal and scope definition phase establishes the purpose of the study, the functional unit, the system boundaries, the required data quality, and the allocation procedures to be applied. The life cycle inventory (LCI) phase involves the systematic collection of data on resource inputs, intermediates, auxiliary materials, energy consumption, emissions, and waste streams. These data are used to construct mass and energy balances that describe the system and to determine the elementary input and output flows, including the application of allocation methods where relevant. The life cycle impact assessment (LCIA) phase converts these elementary flows into potential environmental impacts by applying characterization factors and organizing them into impact categories, such as global warming expressed in kilograms of CO_2-equivalent. Finally, the interpretation phase evaluates the outcomes of the LCI and LCIA, identifies the most influential contributors to environmental impacts, and assesses the robustness of the analysis through sensitivity and uncertainty evaluations.

2.4.1. Goal and scope definition

The system under study is a lab-scale process for recovering cobalt from LCO cathode scrap. The corresponding LCA aims to identify the unit processes that contribute most significantly to potential environmental impacts across the selected impact categories. As suggested by Arvidsson et al., because the environmental assessment is conducted prior to scale-up at a low Technology Readiness Level (TRL), this study can be classified as an early-stage or lab-scale LCA [46]. Accordingly, several limitations commonly associated with lab-scale LCA studies arise. In particular, energy-related impacts tend to be overestimated due to the inherently low efficiency of lab-scale unit operations, which do not take advantage of energy recovery opportunities, such as heat released during reactions or physicochemical processes like dissolution in a solvent. Consequently, this study is not intended for comparison with other processes delivering the same function, but rather to inform researchers involved in process development, supporting eco-design efforts and identifying where optimization efforts should be focused. This study also represents a case of *waste LCA*, as it focuses exclusively on the End-of-Life phase of the component treated and assumes that the material entering the recycling system is burden-free, in line with the zero-burden assumption [47,48].

In waste LCA studies, the functional unit can be defined in different ways depending on the primary function of the process or the aspect to be emphasized [48]. In this study, an output-based functional unit of 1 g of cobalt hydroxide was selected (which also corresponds to reference flow), thereby emphasizing the ability to recover a valuable product from an end-of-life material. Cobalt hydroxide was selected, rather than the cobalt oxide/hydroxide mixture in order to be more conservative.

The system boundary encompasses all unit processes from the shredded virgin cathode scrap through to the drying of cobalt hydroxide, the final product of the process. Accordingly, the following stages are explicitly excluded: upstream extraction, production, and transport of the materials required to manufacture the cathode, transport of cathode scrap from the production site to the research laboratory, any further transformation of the recovered cobalt hydroxide for subsequent applications and its downstream use and end-of-life stages. Lab-scale activities deemed not relevant to the goal of the study, such as fume hood operations or the use of consumables, were likewise excluded from the system boundaries.

Foreground data describing the recycling system were collected directly from laboratory experiments. Background processes were modelled using datasets from the ecoinvent database (v. 3.11) [49], selected to ensure the highest possible degree of geographical and technological representativeness, as verified through the supporting documentation and by prioritizing market datasets representative of the region in which the process was developed. Data gaps were addressed through consultation of the scientific literature and, where necessary, by constructing original datasets [50]. For the model construction and impact quantification, the SimaPro software (version 10.2.0.0) was used. For the assessment of data quality and derivation of the associated uncertainty, the quality pedigree matrix, proposed by (Weidema and Wesnæs, 1996), was used [51]. This method evaluates five aspects related to each data: reliability, completeness, temporal correlation, geographical correlation, and technological correlation.

2.4.2. Life cycle inventory

Masses or volumes of substances and mixtures used as inputs, intermediate mixtures, wastes, and products and co-products in output were measured and reported. Furthermore, energy consumption was evaluated on site using a smart meter, a device that allows real-time monitoring of energy consumption. In cases where the same instrument was used repeatedly for the same period of time, only one measurement was performed, e.g., in the case of centrifugation. For prolonged equipment use, particularly the oven, energy consumption was measured over a shorter period and then scaled to the total operating time, assuming constant temperature. We also followed the methodology proposed by Rossi et al. [52], allocating, when feasible, the energy consumption to the volume occupied by the reagent within the instrumentation (such as, for example, during heating in the oven). On this matter, a sensitivity analysis was carried out to see how impacts change without the energy allocation factor.

After on-site data collection, the data were reorganized and

processed. A spreadsheet was created containing all the collected data, divided by stage (Figure S2), each further subdivided into inputs and outputs, in order to proceed with the calculation procedures. Based on the operational procedure, the process flow sheet was divided into 13 stages representing individual unit processes. Once the inventory was completed (more details on Supplementary Material, Table S1-S15), the reference flow was scaled linearly to fulfil the function of the process (1 g of cobalt hydroxide as an output).

Since LCI data for choline chloride and triethyl phosphate production process is not available in the database, processes were modelled according to commercial patents (CN103374028A; CN1078231A), following an industrial scale-up framework [53–55].

A dataset related to the production of oxalic acid was also built to carry out a sensitivity analysis later on in the study (see Table S16 of the Supplementary Material). The dataset built was adapted from the dataset available in IDEA database named "oxalic acid dibutyl ester {JP} | 163239152pJPN | U" [56]. In the original dataset the final product is dibutyl oxalate but oxalic acid can be obtained through hydrolysis, thus recovering in the organic phase butanol. Separation was modelled by adding water to the dataset and assuming a 95% success of butanol recovery, following methodology suggested by (Hischier et al., 2005) [57]. Emissions to air were calculated from input flows, as the original dataset does not contain any information about it.

In process units where a complete inventory was available, the mass balance check enabled the calculation of any material losses, which were subsequently treated as waste. In process units with missing data (for example, air emissions during oven operations), the missing quantities were assumed to originate from reactions occurring within the unit process or from physical phenomena such as evaporation, thereby satisfying the mass balance.

2.4.3. Life cycle impact assessment

ReCiPe 2016 method was selected to evaluate the environmental performance of the process [58]. It covers a wide range of environmental concerns, making it suitable for supporting eco-design of the process under study. Within the LCIA phase, elementary flows are translated into potential environmental impacts through impact indicators positioned along the cause–effect chain. Two main levels of indicators are commonly distinguished: midpoint and endpoint indicators. Midpoint indicators represent intermediate environmental mechanisms occurring between the emission or resource extraction and the final damage, such as climate change, acidification, or eutrophication. They quantify the potential contribution of a product system to specific impact pathways and are generally characterized by lower model uncertainty and higher scientific robustness, although their direct interpretability in terms of environmental damage is limited. Endpoint indicators, in contrast, are located further downstream in the cause–effect chain and aggregate midpoint results into damage-oriented metrics related to Areas of Protection, such as human health, ecosystem quality, and natural resources. While endpoint indicators provide results that are more directly relevant for decision-making and sustainability interpretation, they rely on additional modelling assumptions and therefore entail higher uncertainty. The combined use of midpoint and endpoint indicators within LCIA allows for both a mechanistically sound assessment of environmental interventions and a damage-oriented interpretation of their potential consequences.

3. Results and discussion

3.1. Recovery of LCO BM from LCO electrode scraps via triethyl phosphate (TEP)

Table 1 reports the mass balance of the TEP-assisted separation applied to LCO electrode scrap. From an initial mass of 17.97 g, 13.16 g of black mass and 2.97 g of aluminium foil were recovered. The recovered aluminium suggests an initial black mass content of about 15 g, corresponding to a recovery yield of 87.7%. This confirms the efficiency of the TEP treatment in enabling effective separation of the active material from the current collector.

Considering the amount of recovered Al, it can be postulated that the mass of BM present in the pristine electrode was 15 g. Hence the recovered BM percentage resulted 87.7%, demonstrating the effectiveness of TEP in promoting binder dissolution and facilitating electrode separation.

Powder X-ray diffraction (PXRD) analysis was employed to assess the crystalline structure of the LCO electrode scrap and the corresponding recovered BM powders. Fig. 3a compares the powder XRD patterns of the pristine BM mechanically detached from the LCO scrap (red line, LCO scrap) and the BM recovered by TEP treatment. (blue line, LCO recovered). The diffraction peaks at $2\theta = 18.9^\circ$, 37.4°, 38.4°, 39.1°, 45.2°, 49.4°, and 59.1° are attributed to the (003), (101), (006), (012), (104), (051), and (009) planes of $LiCoO_2$ hexagonal crystalline phase, (reference code ICDD 96–450–5483). As observed, the diffraction profiles exhibit identical peak positions and relative intensities, indicating that the crystalline structure of LCO remains intact after the TEP treatment.

Thermogravimetric analysis (TGA) was performed to evaluate the percentage of active material, binder (PVDF) and carbon additive in the pristine and recovered BMs, as well as the recovery efficiency. Fig. 3b presents the TGA curve, under O_2, of the pristine BM, mechanically detached from the LCO electrode scraps. Two major weight losses were observed: a first loss of approximately 6% between 350–500 °C, attributed to PVDF binder decomposition [59], and a second loss of about 3% between 500–650 °C, corresponding to carbon additive degradation [60]. Accordingly, the active LCO material content results in roughly 91% of the total black electrode mass (aluminium current collector excluded). Fig. 3c shows the TGA profile of the LCO powder recovered using TEP. The signal related to PVDF is no longer present, confirming the complete removal of binder materials during the recovery process. Only a mass loss of 1.75% above 500 °C can be observed which corresponds to a carbon additive residue. Thus, it can be inferred that the recovered material comprises approximately 98.25% pure $LiCoO_2$.

Table 2 presents the quantitative analysis of cobalt and lithium concentrations in both the pristine production scraps and the recovered BM, as determined by MP-AES. The elemental composition of the recovered LCO material after TEP treatment shows slightly higher cobalt and lithium contents (510.9 and 82.6 mg g^{-1}, respectively) compared to the pristine BM scraps (481.5 and 78.02 mg g^{-1}, respectively). This difference can be attributed to the mechanical scraping of the BM from the current collector in the pristine samples, which results in partial contamination with aluminium species. Consequently, the initial mass of the pristine LCO scraps includes both active electrode material and small amounts of aluminium from the current collector, leading to an apparent dilution of the measured Co and Li concentrations relative to the recovered LCO.

Table 1
Summary of the mass balance obtained during the TEP-based separation of the black mass from the current collector for $LiCoO_2$ (LCO) electrode scrap.

LCO scraps mass (including Al current collector) (g)	TEP (mL)	TEP solvent (g)	TEP including carbon and binder (g)	Recovered black mass powder (g)	Recovered black mass powder (%)	Recovered Al foil (g)
17.97	180	192.6	174.15	13.16	87.7	2.97

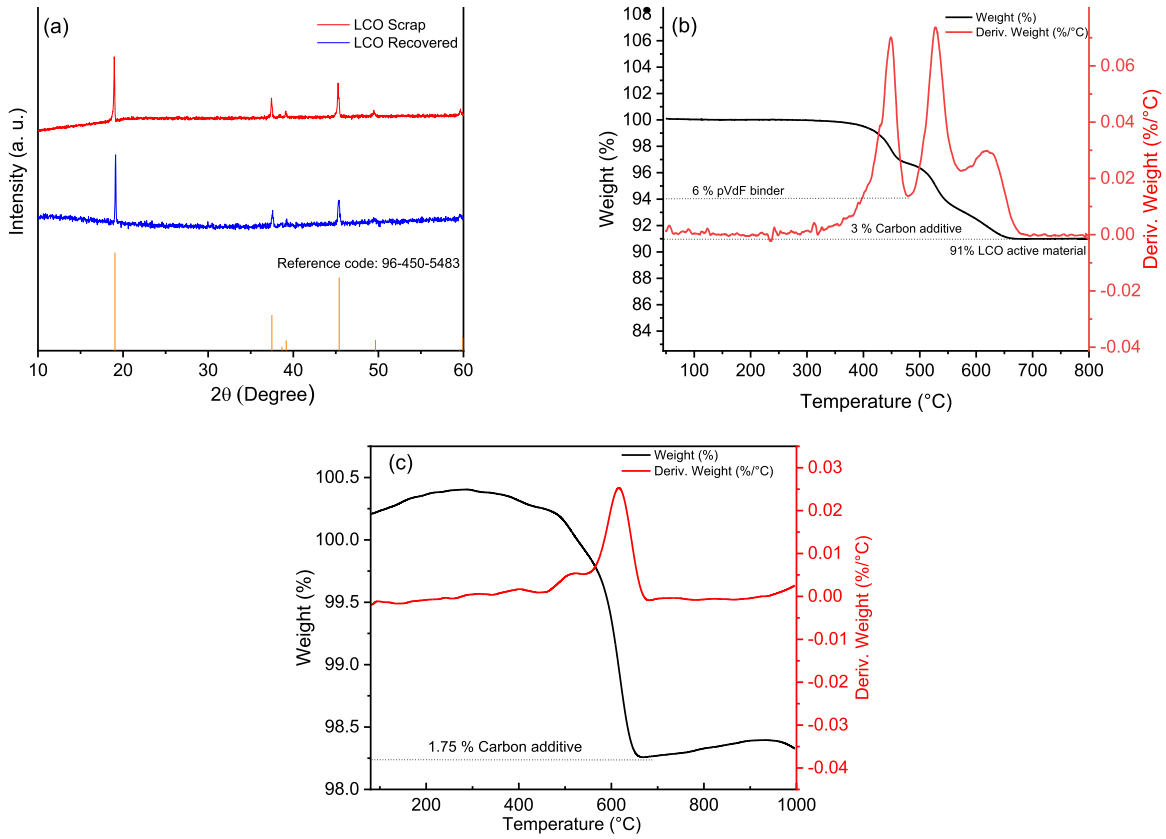

Fig. 3. (a) comparative powder XRD analysis of the pristine BM mechanically detached from the LCO scrap (BM, mechanically detached, red line) and the BM recovered by TEP treatment (BM recovered by TEP, blue line). TGA curves of (b) mechanically and (c) TEP-recovered BM powder from LCO scraps.

Table 2
Analysis via MP-AES of cobalt and lithium concentration in mechanically and TEP-recovered BM from LCO production scraps. The data are expressed in mg per g of BM.

BM Samples	Concentration (mg g^{-1})	
	Co	Li
Concentration (RSD%)		
Mechanically recovered	481.5 (1.76%)	78.0 (0.79%)
TEP recovered	510.9 (0.13%)	82.6 (0.21%)

3.2. BM leaching by DES and cobalt recovery

During the leaching process, the choline chloride–oxalic acid DES provides both the chemical environment and the reactive species required for $LiCoO_2$ dissolution. Choline chloride functions as the hydrogen-bond acceptor, forming the eutectic liquid and facilitating the transport and stabilization of dissolved metal ions by chlorine complexation. Oxalic acid acts as the hydrogen-bond donor, generating an acidic medium that promotes proton-assisted disruption of the $LiCoO_2$ lattice while simultaneously providing oxalate ligands that coordinate dissolved cobalt species, thereby shifting the dissolution equilibrium toward metal extraction [61,62]. Following leaching, W. Ma et al. have shown that cobalt–oxalate complexes readily undergo hydrolysis in aqueous media, releasing Co^{2+} species whose coordination environment is strongly pH-dependent [40]. In particular, increasing water content weakens cobalt–oxalate coordination and promotes ligand exchange, as demonstrated by the hydrolysis and dissociation of cobalt–oxalate precipitates into aqueous Co^{2+} species [40]. Under the highly alkaline conditions employed in this work (5 M KOH, pH ≈ 12), the released Co^{2+} preferentially coordinates with hydroxide ions, leading to the displacement of oxalate ligands and the precipitation of cobalt (II) hydroxide [Co $(OH)_2$] or oxides.

As described in 2.2.2, after DES-leaching, the pH of the dark green viscous liquid was progressively increased. A distinct colour transition from dark green to purple, violet, and finally brown was observed as the pH increased (Figure S1).

Fig. 4a reports the powder XRD patterns of the powder obtained at pH 12 and confirms the formation of a crystalline phase. The diffraction peaks located at 2θ = 19.1°, 32.5°, 38°, 51.5°, 58° and 61.7° correspond to the (001), (010), (011), (012), (110) and (111) planes of CoO_2 (reference code 96–900–9102) and $Co(OH)_2$ (reference code 96–101–0268). Hence, we can argue that the recovered powder could be a mixed phase of hydroxide and oxides. The absence of significant impurity peaks in the powder XRD spectra confirms the effective removal of residual compounds, including triethyl phosphate and potassium oxalate during cobalt recovery from LCO electrode scraps.

The powder purity was further assessed by TGA that was performed in O_2 flow in order to detect the presence of any organic or carbon residue. The TGA curve of the recovered cobalt compound powder reported in Fig. 4b exhibits two distinct weight loss events that indicate that the main component is a mixed hydroxide/oxide cobalt powder. Indeed, it reflects the sequential dehydration and desorption of oxygen from CoO_2. The pronounced weight loss near 200 °C can be associated both to dehydration of Co $(OH)_2$ to cobalt oxide and to the conversion of CoO_2 into CoO(OH) and Co_3O_4 [63]. The mass loss at ca 850°C can be related to the transformation of Co_3O_4 into CoO [63–65]. The total weight loss of approximately 0.88% indicates a minimal residue originating from the ChCl–OA DES system.

The cobalt and lithium content in the recovered cobalt oxide/hydroxide and in the supernatant liquid phases obtained from DES treatment at pH 12 was evaluated by MP-AES. Specifically, Table 3 reports the concentrations of cobalt and lithium in the recovered cobalt oxide/hydroxide, and in the supernatant solution before (S1) and after

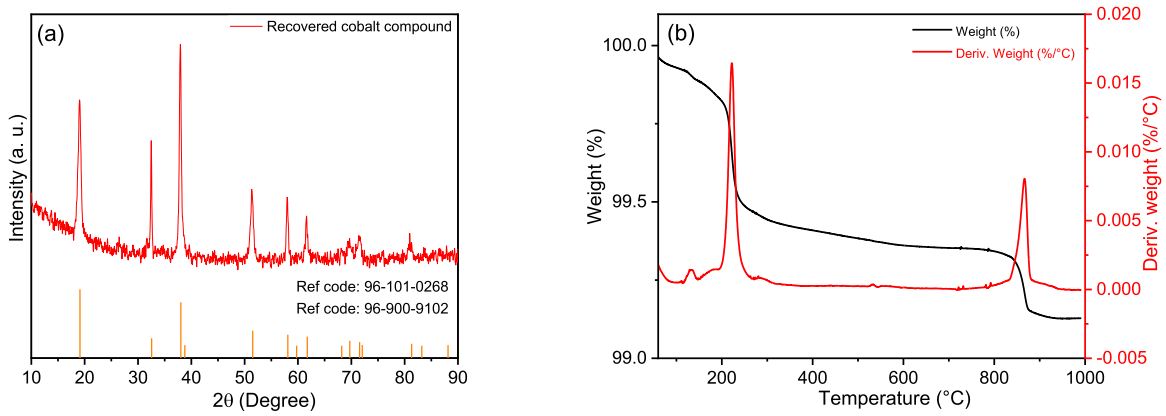

Fig. 4. (a) Powder XRD patterns of the cobalt compound obtained by DES leaching and precipitation at pH 12, with the reference codes for $Co(OH)_2$ (96–101−0268) and CoO_2 (96–900−9102) and (b) TGA curve of the cobalt compound powder recovered after LCO BM leaching with DES.

Table 3
Quantitative determination of cobalt and lithium by MP-AES in the recovered cobalt oxide/hydroxide and in the liquid phases obtained from DES treatment at pH 12: S1 (solution prior to centrifugation), S2 (supernatant after precipitation and first centrifugation), and S3 (washing solution of the precipitate).

Samples	Concentration (mg g^{-1})	
	Co	Li
Concentration (RSD%)		
Recovered cobalt oxide/ hydroxide	499.3 (1.03%)	0.0 (4.51%)
Solution S1	0.0 (8.66%)	0.15 (1.68%)
Solution S2	0.0 (9.42%)	0.16 (0.40%)
Solution S3	0.0 (10.07%)	0.005 (1.42%)

centrifugation (S2), and in the solution collected from the washing step of the precipitate (S3). Notably, lithium is present only in the liquid phases, while cobalt is present only in the solid precipitate. This confirms the effective separation of cobalt and lithium during the DES treatment at pH 12. We attempted to recover Lithium, by using CO_2 and Na_2CO_3 to form Li_2CO_3. At first, we successfully experimentally simulated the process with synthetic solutions, then we applied the process to our real wastes. Unfortunately, in the latter case we were unable to precipitate Li_2CO_3 because it requires a Li^+ concentration above approximately 5 g L^{-1} , which is one order of magnitude higher than the value that we reached in our system. Indeed, the MP-AES data reported in Table 3, indicates that the total Li in the solution from DES is 0.341 g/L.

Table 3 reports an amount of Co that is 77% than the theoretical stoichiometric value expected for CoO_2 (648 mg of cobalt per g of CoO_2). This might be due to a not complete extraction of Co during sample preparation for MP-AES.

The overall cobalt mass balance was evaluated by considering the cobalt initially present in the TEP-recovered black mass and the amount recovered as cobalt oxide/hydroxide after DES leaching and precipitation. From MP-AES analyses, the content of cobalt in 1.0 g of recovered black mass containing is 510.9 mg g^{-1} (Table 2). After DES leaching and subsequent precipitation, 459 mg of cobalt oxide/hydroxide was obtained, corresponding to approximately 290 mg of cobalt, which brings about an overall cobalt recovery efficiency of 57% ± 10% (RSD, n = 3). Such a low recovery efficiency is mainly attributed to material losses occurring during multiple laboratory-scale processing steps, including separation of solid residues after leaching, centrifugation, washing, and transfer of viscous DES-containing solutions. These losses are particularly relevant at low Technology Readiness Level (TRL), where process handling is not yet optimized and recovery operations are performed on a small scale. Importantly, the high purity of the recovered cobalt hydroxide confirmed by XRD and TGA indicates that the limitation is primarily related to material recovery and process handling rather than ineffective cobalt dissolution or precipitation chemistry.

Hence, the 57% efficiency is not limited by chemical boundaries but is a typical artifact of low Technology Readiness Level (TRL) material handling at the laboratory scale (losses during sequential filtration, multiple washings, and transferring viscous liquids). Quantified lab-handling mass losses have been systematically tracked in the LCI tables (Table S1-S15).

Table 4 summarizes representative literature on cobalt recovery from Co-based cathode materials, both powders and spent LIBs, using both conventional mineral acid leaching and DES-based approaches, together with the operating conditions and recovery/extraction efficiencies.

The comparison highlights that conventional concentrated mineral acid systems and several DES-based processes often report cobalt recoveries above 90%. However, these studies differ substantially from the present work in several important aspects. Most literature reports evaluate leaching efficiency from cathode powders, both pristine active materials, while we are processing real cathode scraps, that include current collector and BM. In addition, the reported works frequently employ elevated temperatures (110–170 °C), hydrothermal reactors, concentrated mineral acids, oxidizing/reducing agents, microwave-assisted process or electrochemical deposition [40,66–71]. In contrast, the present study processes LCO production roll scraps using green solvents and circum-ambient conditions (55 °C and atmospheric pressure).

3.3. Life cycle assessment (LCA) of the cobalt recovery process

The results were obtained at both the midpoint and endpoint levels, to gain better insight into how the different process steps influence the final environmental impacts. LCIA results in absolute values obtained are reported in Table S17 and Table S18 of the Supplementary Material.

To visualize and highlight the environmental hotspots of the system, a heat map (Fig. 5) for each level was developed. Please note that some process units have similar operations (e.g., centrifugation steps) though they were not grouped together because the units considered involve different amounts and types of inputs. The heat map at the midpoint level (Fig. 5a) shows that Step 5 (Preparation of the DES solution) carries the most impacts for all categories except for Ionizing Radiation (IR, 7.39%), Mineral Resource Scarcity (MRS, 17.69%) and Water Consumption (WC, 16.62%). This step is also the only one to carry more than half the overall impact of a category, namely for Stratospheric Ozone Depletion (SOD), Ozone Formation – Human Health (OFHH), Fine Particulate Matter Formation (FPMF), Ozone Formation – Terrestrial Ecosystems (OFTE) and Terrestrial Acidification (TA).

In the Global Warming (GW) category, Steps 5, 6, 10, and 12

Table 4
Comparison of cobalt recovery from Co-based cathode materials using conventional acid leaching and DES-based approaches.

Feedstock	Leaching system	Operating conditions	Cobalt recovery / extraction efficiency	Ref.
NMC622 powder from spent LIB	1 M H_2SO_4/H_2O_2	Acid leaching with oxidant assistance	~50.6% Co extraction	[66]
Spent LIB LCO cathode powder	3 M H_2SO_4/H_2O_2	Acid leaching with oxidant assistance, 70 °C	99.50% Co recovery	[67]
Fresh $LiCoO_2$ cathode powder	Choline chloride:ethylene glycol DES	Optimized ChCl:EG (1:5), 160 °C, 48 h, followed by Co electrodeposition	maximum faradaic efficiency of about 80% for cobalt deposition.	[68]
Spent LIB cathode powder	Choline chloride:ethylene glycol:benzoic acid ternary (1:1.6:0.4) DES	Optimized at 443.15 K (~170 °C), 3 h	~100% Co leaching efficiency	[69]
Fresh $LiCoO_2$ cathode powder	Choline chloride:citric acid:H_2O DES	Water-assisted DES leaching using a hydrothermal reactor	99.76% Co recovery after precipitation	[70]
Spent LIB LCO cathode active material powder	Ethylene glycol:sulfosalicylic acid dihydrate (12:1) DES	110 °C, Hydrothermal autoclave, 6 h	93.5% Co leaching efficiency	[71]
Lithium cobaltate LCO powder	Choline chloride:Oxalic acid (1:1) with water	Cobalt oxalate recovery Using a Microwave-Assisted DES	99.21% Co recovery in form of Cobalt oxalate	[40]
LCO production roll scraps	Choline chloride:Oxalic acid DES (1:1)	55 °C, 48 h, KOH precipitation	57% Co recovery	This work

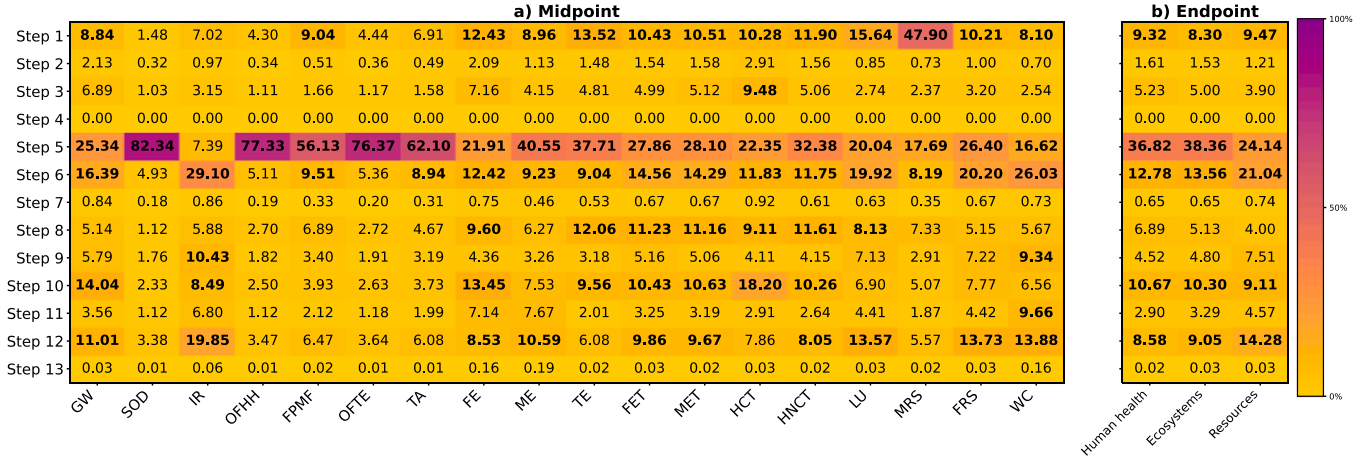

Fig. 5. Heat map showing the LCIA results *(in %)* of the selected impact categories*, both for a) midpoint and b) endpoint categories.* Step 1: Black mass separation with TEP; Step 2: Removal of TEP from black mass; Step 3: Washing of black mass; Step 4: Black powder drying; Step 5: DES preparation; Step 6; Leaching in DES of the black powder; Step 7: Separation of DES from solid residues; Step 8: KOH solution preparation; Step 9: pH adjustment with KOH; Step 10: Separation of precipitate from supernatant; Step 11: Precipitate washing; Step 12: Removal of potassium oxalate; Step 13: Drying of cobalt hydroxide. Values in bold are those contributing more than 8% to the environmental impacts, for a specific impact category.

contribute approximately 67% of the total impact. Although materials in DES preparation play a key role, the contribution of the other three process units increases significantly due to the involvement of hazardous waste treatment. For the IR category, steps bearing the greater burden are Steps 6, 9 and 12, accounting for nearly 60% of the overall impacts. These phases are associated with the greatest energy consumption among all unit processes; the reason behind this can be attributed to the share of nuclear energy (imported mainly from France) present in the Italian electricity mix.

Interestingly, Step 1 (Black mass separation with TEP) carries less than 16% of the environmental burden in all categories except for MRS, where it contributes for around 48%. This is mainly due to the extraction and processing of phosphate rock, used in the production of phosphorous chloride, raw material for TEP.

Steps 4 and 13 both involve drying operations and still carry the least of impacts across all categories. These results are influenced by the allocation rule applied, following (Rossi et al., 2024), with energy consumption allocated by volume occupied by the sample.

A sensitivity analysis was also performed to verify this assumption, reported in Figure S4 in Supplementary Material, with the oven energy consumption considered as a whole. This confirmed the robustness of the model since the most impactful process phases remained the same even after reducing the allocation factor. The endpoint-level heat map (Fig. 5b) confirms the trends previous stated, with Steps 5 and 6 being the first and second most impactful, respectively, followed by Steps 1, 10 and 12 contributing between around 8% and 14% across all endpoint categories.

For these process units a contribution analysis was carried out to understand which type of flows are responsible of the greater environmental burden. To obtain aggregated results for each process unit considered normalization and weighting were applied to the LCIA results; the outcomes expressed as percentages are shown in Fig. 6.

Steps 1, 5 and 6 represents the units carrying the process innovations, involving the use of triethyl phosphate and the Deep Eutectic Solvent constituted of choline chloride and oxalic acid, as these represent the innovative reagents selected by the research group. This highlights that future efforts to optimize the process should be concentrated on the reuse and recycling of these solvents. Steps 10 and 12 both involve centrifugation operations and the disposal of residuals, which were modelled as being sent to treatment.

Within the "BM separation with TEP" unit, the production of triethyl phosphate (TEP) accounts for 92.2% of the total environmental impact associated with this phase. Tracing the upstream supply chain, the dominant contributors to the solvent's overall impact are the raw materials required for its synthesis, specifically ammonia, phosphorus chloride, and ethanol. No credit was allocated for the aluminium recovered during this process unit, as it requires additional treatment steps before it can reach a marketable grade. Although material losses

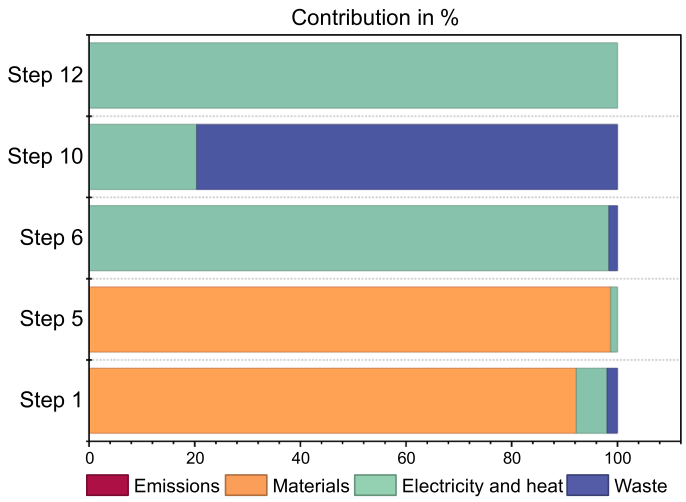

Fig. 6. Contribution analysis of the most impactful stages. Percentages displayed for each step represent the contribution of a corresponding flow to the total endpoint impacts, aggregated in a single score fashion. In Step 1, emissions contribute for 5.70E−5% of the total impacts.

were assumed to arise entirely from TEP evaporation, the resulting emissions appear to contribute only marginally to the overall impact profile.

Within the unit "DES Preparation", the main environmental hotspots are represented by the production of oxalic acid and choline chloride, contributing for 75% and 23%, respectively, to the total unit process impact, across all categories. The high contribution of materials in Phases 1 and 5 was verified through additional contribution analyses related to the synthesis of the three substances, showing that their impacts in turn derive from the raw materials used for their synthesis.

In Step 6, the only input to this phase, besides the BM from the previous stage, is electricity. Consequently, the contribution analysis results consistently show that electricity accounts for 98.4% of the total impact of this step. As already mentioned in the Goal & Scope definition of the study, for lab-scale processes electricity consumption can often mask the impact of other flows, since when scaling up, the energy demand of unit processes tends to decrease while efficiency increases. Nevertheless, the electricity consumed in step 6 is associated with maintaining the leaching operations at 55°C for 48 h, resulting in a significant energy demand. Therefore, improving process kinetics and reducing reaction time should be a priority.

For Steps 10 and 12, although they involve the same type of operation, i.e., centrifugation, the impact profiles differ significantly. In Step 10, 79.6% of the impacts arise from waste disposal, whereas in Step 12 electricity generation accounts for almost all impacts. This difference is due to the nature of the output streams handled in each step. In Step 12, the supernatant obtained after centrifugation consists mainly of water and was modelled as being sent to a wastewater treatment plant. In contrast, in Step 10 the solid fraction containing cobalt is separated from the supernatant bearing lithium. At the time of writing, lithium recovery had not yet been optimized; therefore, this liquid stream was treated as hazardous waste destined for incineration.

Sensitivity analyses were conducted to assess the robustness of the developed model and to explore possible strategies to mitigate process hotspots. First, based on the contribution analyses, potential solutions were hypothesized to reduce the criticalities of the most impactful phases.

For Phase 6, instead of the actual Italian electricity mix, a mix was created by increase of + 20% the renewable sources in the IEA (International Energy Agency) 2023 electricity mix for Italy, representing a future scenario with a higher share of renewable energy. Figure S3 shows that this variation resulted in a 37.7% reduction in the total impact of the phase. At the midpoint level, a decrease in the scores for global warming, fine particulate matter formation, and fossil resource scarcity was observed, due to the lower use of fossil-based energy. Conversely, some impact categories (e.g. terrestrial ecotoxicity) showed an increase in environmental effects, indicating a partial burden shifting from one impact area to another.

A review of the ecoinvent documentation for the oxalic acid production dataset in China revealed that the industrial process selected for modelling, i.e. the oxidation of propylene, represents an outdated route that has been largely superseded in practice. Current industrial methods for oxalic acid production in China primarily include the CO coupling method, the ethylene glycol oxidation method, and the sodium formate method. To account for this limitation, an alternative dataset from the IDEA database was adapted to perform a sensitivity analysis [56], examining how impacts vary for the process Step 5 across all midpoint and endpoint categories, alongside a direct comparison between the two datasets. Results are reported in the form of a heat map in Fig. 7.

The DES preparation step remains one of the greatest contributors to overall impacts, although its relative contribution decreases compared to the analysis in Fig. 5, particularly for SOD, OFHH, FPMF, OFTE, and TA. Step 6 emerges as the dominant phase across most categories, and for all endpoint categories, while Step 5 ranks second, with the exception of ME and TE (and marginally for OFHH, FPMF, and HCNT, where differences are within a few decimal points). This confirms the role of electricity consumption in the development of this process and likely constitutes the main obstacle to its scale-up.

Finally, an uncertainty analysis of the entire process was carried out using the Monte Carlo method, assuming a lognormal distribution with a 95% confidence interval over 100 iterations (Table S19 in the Supplementary Material) [72]. Most midpoint categories exhibit a coefficient of variation (CV) between 5.6% and 18%, while six categories (FE, FET, MET, HCT, LU, and MRS) show higher values ranging from 27.2% to 39.7%. IR, WC, and HNCT display outlier CV values, which can be attributed to the intrinsic uncertainty associated with certain elementary flows linked to these categories [48].

Model's robustness was confirmed by comparing the results obtained with the chosen impact method (ReCiPe 2016) and an alternative method (Environmental Footprint 3.1), shown in Table S20. Categories with the same unit of measurement were compared, minor differences in results (e.g., global warming ±1.94%), except for *water consumption* category. The observed difference can be attributed to the characterization factor used in the different impact assessment methods. The EF 3.1 impact assessment method quantifies water consumption in relation to the water scarcity of the specific geographic region, according to the AWARE (Available WAter REmaining) model. This model assesses the amount of water remaining in a watershed after meeting the demands of

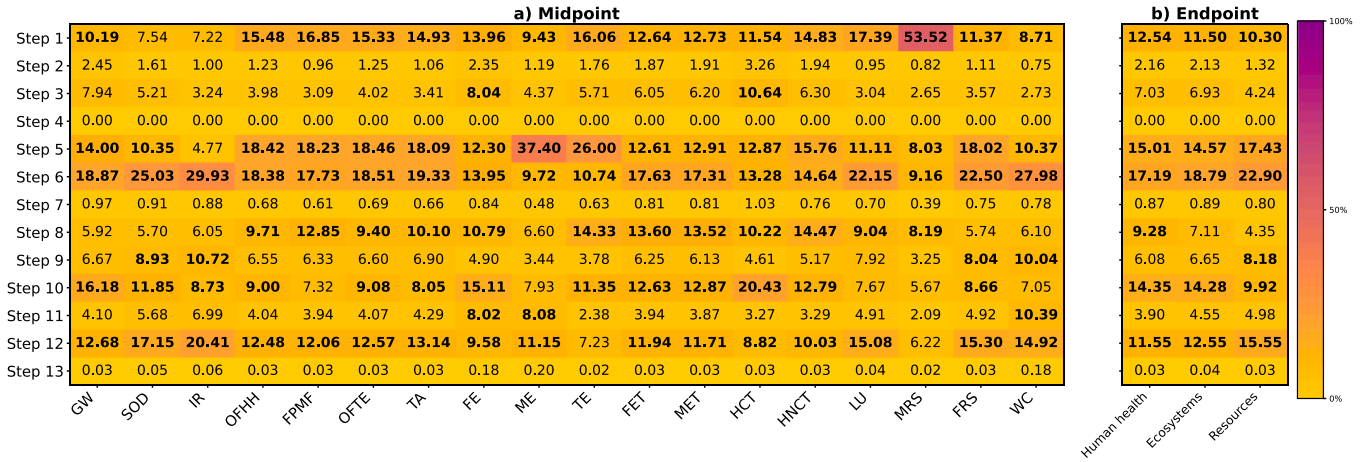

Fig. 7. Heat map showing the LCIA results (in %) of the selected impact categories, both for a) midpoint and b) endpoint categories. Oxalic acid production original dataset from ecoinvent was replaced with one adapted from IDEA database (see Table S16 for further information).

humans and aquatic ecosystems. In contrast, the ReCiPe 2016 method is based on different models, including those developed by Döll and Siebert (2002) and Hoekstra and Mekonnen (2012) [58,73]. In this approach, water consumption may either coincide directly with the life cycle inventory flows or depend on the efficiency of water use in relation to the type of activity considered.

In order to identify opportunities for improving the process's environmental performance and highlight key areas for optimization, a simplified prospective LCA was carried out [46]. Lab-scale LCAs are particularly useful for identifying hotspots at early stages of technology development, thereby guiding optimization efforts [74]. Meanwhile, prospective modeling allows early-stage processes to be evaluated at a future, more mature scale (e.g., large-scale production). Based on the previous discussion, the main drivers of environmental impacts are the consumption of chemicals, even those deemed green and sustainable, and the energy required during the leaching phase. While TEP and DES remain promising solutions, their recycling and reuse must be carefully evaluated. In the lab-scale process, the unreacted TEP contains binder and graphite, which must be removed prior to recycling. A microfiltration step was considered as a potential recovery method. The energy demand for this operation was estimated consulting the framework proposed by Piccinno et al. (2018) [53].

Due to the lack of empirical data on actual recovery efficiency, several scenarios were developed to assess how variations in efficiency affect environmental impacts. Depending on the recovery rate, both the raw chemical inputs and the amount of material sent to hazardous waste incineration vary accordingly. Regarding the DES, direct reuse was evaluated; according to Li et al. (2023) [75], DES can be reused for cobalt leaching at least four times before the lithium concentration in the leachate reaches saturation, preventing further Co extraction. Although DES is reused, a make-up fraction of oxalic acid – acting as both a reducing agent and a complexing agent – must be added to compensate for the amount required to reduce all Co^{3+} to Co^{2+} [76,77]. Similar to TEP, the impacts were calculated across multiple DES reuse cycles to observe variations across different impact categories.

Overall, 24 alternative scenarios were evaluated alongside the baseline. Fig. 8 highlights the results for Global Warming and Mineral Resource Scarcity, while the remaining impact categories are provided in Table S21 of the Supplementary Material. For Global Warming, reusing DES proved to be the most effective strategy to reduce the overall environmental burden (achieving a 7.1% impact reduction with just one reuse cycle). Conversely, TEP recycling is advantageous only if recovery efficiency exceeds 70%; below this threshold, the energy demand for microfiltration makes the process even more burdensome. A reverse trend is observed for Mineral Resource Scarcity: TEP recycling consistently offers significant benefits regardless of efficiency, yielding impact reductions ranging from 5.7% (at 30% recovery) up to 16.9% (at 90% recovery). On the other hand, DES reuse reduces impacts in this category by up to approximately 7%. Therefore, process optimization should prioritize the development of efficient recycling and reuse loops for these innovative materials. Nevertheless, as these scenarios rely primarily on literature data, future studies should focus on

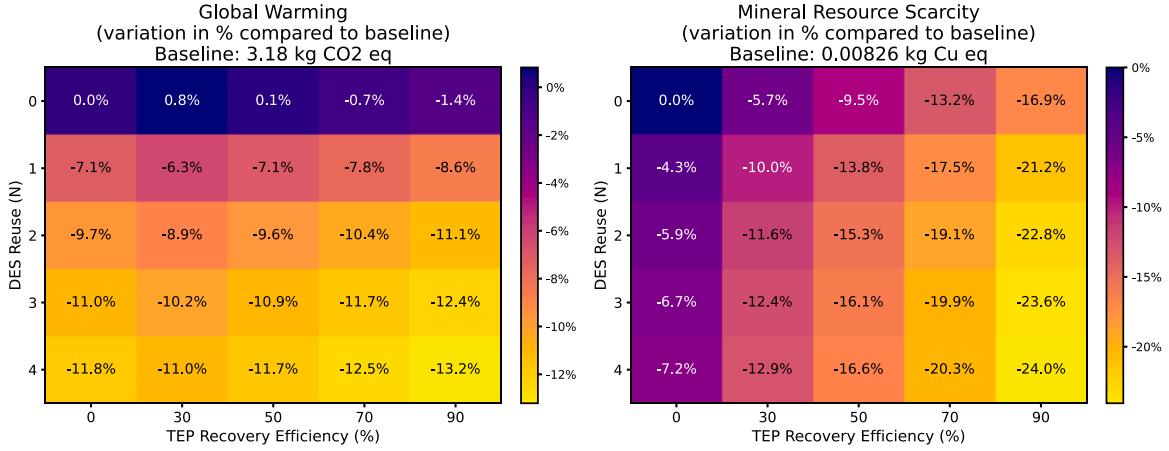

Fig. 8. Variation of the impacts (expressed as a percentage) compared to the baseline scenario, for the categories Global Warming and Mineral Resources Scarcity. Variations are expressed for scenarios in which recovery efficiency for TEP and reuse of DES change across different values.

experimentally verifying the practical feasibility of these recovery operations.

Another major hotspot in the LCO recovery process is the high energy consumption measured during the leaching phase, which reached 1.28 kWh/g at the laboratory scale. Applying the framework proposed by Piccinno et al. (2018) [53], a prospective scale-up model (assuming a 1000-liter reactor) was developed to determine whether this high energy demand stems from heating or from stirring difficulties caused by the high viscosity of DES.

The scaling framework assumes turbulent flow – defined by a Reynolds number (Re) greater than 10000 – to maintain a constant power number (N_p). To verify this assumption for the targeted system, the Reynolds number was calculated using density and viscosity data for this specific DES at 55°C from Popescu et al. (2014) [78]. The resulting value Re = $1.33*10^4$) confirmed that the flow is indeed turbulent, albeit close to the transitional regime boundary. Using Piccinno's equation with an N_p of 0.79, the energy required for stirring was calculated to be 0.75 kWh/kg of cobalt hydroxide. Even under a worst-case scenario with non-turbulent flow and a significantly higher power number ($N_p = 5.5$), the stirring energy demand would be 5.25 kWh/kg, still three orders of magnitude lower than the experimental lab-scale value [53].

Furthermore, heating energy requirements were estimated assuming a specific heat capacity of 2.6 J/kg*K (adapted from Naser et al., 2016 [79]). The calculated thermal energy demand was 0.37 kWh/kg. These findings indicate that in a potential industrial scale-up, energy consumption for stirring will represent a far greater fraction of the energy balance than thermal energy. Overall, reducing leaching time remains the most critical target for minimizing the total energy burden of the process.

One of the main goals of lithium battery recycling is the reduction of virgin mineral extraction [80]. For this reason, the environmental performance of cobalt hydroxide recovery through the recycling process described here was compared with that of primary cobalt hydroxide production. Although the results (Fig. 9) may appear less promising, it is crucial to consider that the process is still at the laboratory scale. Hence, there remains room for improvement, including both optimization of operational parameters and refinement of lithium recovery.

Beyond conventional environmental LCA indicators, reducing primary cobalt extraction may also have broader sustainability implications. From a functional perspective on natural resource use, recycling can support the availability of materials that are essential for socio-economic systems, particularly for Critical Raw Materials such as cobalt [81,82]. However, these aspects relate to supply security and system resilience are not fully captured by environmental LCA, being more appropriately addressed through criticality assessment and within a Life Cycle Sustainability Assessment framework [83].

4. Conclusions

Cobalt can be effectively recovered from LCO cathode scraps by combining the BM detachment from the current collector with TEP and the leaching with choline chloride–oxalic acid. Cobalt can then be recovered by adding KOH to the DES solution and precipitating mixed phase of cobalt hydroxide/oxide. The good recovery yield, together with the reproducibility of the dissolution and precipitation steps, confirms that the DES-based process is capable of extracting cobalt from cathode scraps under mild conditions. These results validate the feasibility of this solvent system as a promising alternative to conventional hydrometallurgical routes for cobalt recovery.

Despite the experimental lab validation as alternatives to classic solvents, DESs are far from being industrially applicable. DES-based systems are characterized by high viscosity and slow leaching kinetics that complicate reliable scale-up modelling. Another issue that remains, [61,76] common to other studies based on the use of DES for hydrometallurgy, is solvent recycling, which still needs to be optimized: lithium remains in the raffinate, and if a recycling stream is developed, an oxalic acid make-up may need to be implemented, since this component can act as an oxidant for cobalt and is therefore consumed.

A limitation of this work is that we considered Lithium-DES solutions as waste because of the lack of experimental data on the lithium recovery at the lab scale. Indeed, we attempted to recover Lithium, by using CO_2 and Na_2CO_3 to precipitate Li_2CO_3, which was not successful due to the low Li^+ concentration (0.341 g L^{-1}, Table 3).

Moreover, the components typically used to formulate DESs are relatively expensive from an economic standpoint – a significant drawback for an industry like the metallurgical one, which traditionally relies on cheap solvents, particularly in cases where the revenue per unit mass of recovered material is low.

This study applied a structured LCA framework comprising goal and scope definition, inventory development, impact assessment, and interpretation to evaluate the environmental performance of a DES–based cobalt recovery process from LCO cathode scraps. By grounding the assessment in ISO 14040/44 standards and employing a cradle-to-gate system boundary, the LCA enabled a transparent evaluation of material and energy flows throughout the laboratory-scale process and provided a systematic foundation for identifying environmental hotspots.

Across the inventory and subsequent impact assessment, solvents and electricity emerged as the dominant contributors to environmental burdens. Despite the motivation for selecting TEP and ChCl–OA DES

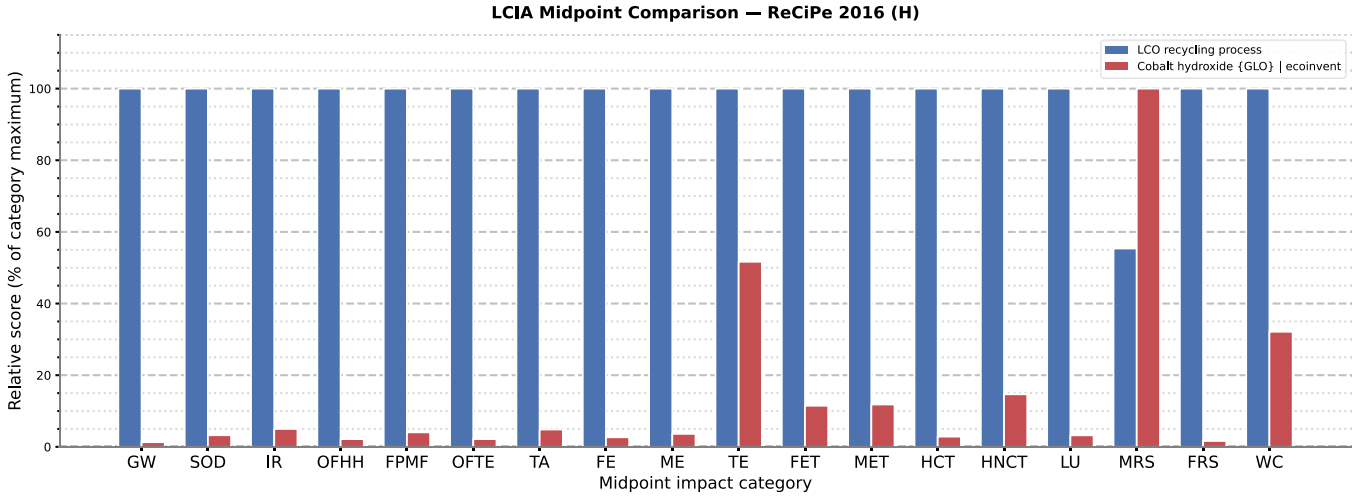

Fig. 9. Comparison between cobalt hydroxide production from the studied process and from primary production.

based on their growing relevance in emerging recycling technologies, their production and use were shown to be consequential drivers of impacts, underscoring the importance of integrating solvent optimization into early process design. Electricity demand, particularly during dissolution and thermal treatments, further highlighted the sensitivity of system performance to regional energy mixes. Consequently, the methodological structure of the LCA clarified how upstream processes such as solvent synthesis and national electricity profiles exert influence on downstream results.

The interpretation phase demonstrated the value of iterative refinement for early-stage technologies. Sensitivity analyses, aligned with the LCA framework, confirmed the model's robustness while illustrating potential mitigation strategies, including solvent reuse and increased reliance on renewable electricity. Complementary methodological checks such as alternative impact assessment methods and Monte Carlo uncertainty analysis reinforced the consistency of the findings and delineated categories where uncertainty remains significant.

Nevertheless, several methodological limitations inherent to early-stage LCA studies were identified. The need to model TEP and choline chloride from primary raw materials due to the absence of database entries introduces uncertainty regarding industrial representativeness. Moreover, laboratory-scale conditions, absent of process optimization, likely overestimate environmental burdens relative to future scaled processes. Additionally, cross-study comparisons remain constrained by discrepancies in functional units and system boundaries within the existing LCA literature on LCO cathode recycling.

Overall, the structured LCA methodology enabled a comprehensive understanding of the environmental profile of this emerging cobalt recovery route and demonstrated how methodological rigor can guide ecodesign in early process development. Future work should integrate simulated or experimental scale-up, explore alternative leaching systems, and incorporate DES, TEP and lithium recovery to enable a more complete assessment of process multifunctionality. Such developments would enhance the robustness of environmental performance evaluations and strengthen the role of LCA as a decision-support tool in advancing sustainable battery recycling technologies.

CRediT authorship contribution statement

Shoayb Mojtahedi: Writing – original draft, Methodology, Investigation, Formal analysis, Data curation. **Leonardo Sparascio:** Writing – original draft, Software, Methodology, Investigation, Formal analysis, Data curation. **Federico Mascetti:** Formal analysis, Data curation. **Salan Xierzati:** Investigation, Formal analysis, Data curation. **Andrea Vitale:** Formal analysis, Data curation. **D'Agostino Simone:** Formal analysis, Data curation. **Chiara Samorì:** Writing – review & editing. **Rombolà Alessandro:** Writing – review & editing. **Greggio Nicolas:** Writing – review & editing. **Daniele Cespi:** Writing – review & editing, Validation, Supervision, Resources, Conceptualization. **Fabrizio Passarini:** Writing – review & editing, Resources. **Chiara Zentile:** Writing – original draft, Software, Methodology, Investigation, Formal analysis, Data curation. **Antunes Staffolani:** Writing – review & editing. **Ncholu Manyala:** Writing – review & editing. **Francesca Soavi:** Writing – review & editing, Validation, Supervision, Resources, Funding acquisition, Conceptualization.

Supplementary material

Additional results are reported in the file "Supplementary Material.docx". The file includes a picture of the cobalt recovery process (Figure S1), the flow diagram of the process (Figure S2), LCI data (Tables S1 to S15), LCI related to production of oxalic acid via CO coupling method, adapted from IDEA database (Table S16), a diagram that illustrates the contribution analysis of the main process phases (Figure S3), the comparison of impact categories within ReCiPe 2016 (Table S17), the midpoint-level results of the process of the Life Cycle Impact Assessment (Table S18), the heat maps of the process (Figure S4), and the results for Monte Carlo uncertainty analysis for the entire process (Table S19) a comparison of the results of three impact categories within the ReCiPe 2016 and Environmental Footprint 3.1 impact assessment method (Table S20), a variation of the impacts compared to the baseline scenario, by modifying efficiency recovery values for TEP and number of reuses for DES (Table S21).

Funding

We acknowledge for financial support the projects: "RELY: Transformation of REcovered/recycled spent Lithium-ion BatterY cathodes into porous materials for high power-energy storage" (MAECI-Italy South Africa Grande Rilevanza bilateral project); "DiGreen: a digital and chemical approach for green recycling of Li-based batteries" funded by the European Union - Next Generation EU, Missione 4 Componente 1 Project CUP J53D23008790006

Declaration of Competing Interest

The authors declare that they have no known competing financial interests or personal relationships that could have appeared to influence the work reported in this paper.

Appendix A. Supporting information

Supplementary data associated with this article can be found in the online version at doi:10.1016/j.jece.2026.124661.

Data availability

All data are available in the manuscript and supporting information

References

[1] Md.D. Ahmed, K.M. Maraz, Revolutionizing energy storage: overcoming challenges and unleashing the potential of next generation lithium-ion battery technology, Mater. Eng. Res. 5 (1) (2023) 265–278, https://doi.org/10.25082/MER.2023.01.003.

[2] A.I. Stan, M. Swierczynski, D.I. Stroe, R. Teodorescu, S.J. Andreasen, Lithium ion battery chemistries from renewable energy storage to automotive and back-up power applications - an overview, *OPTIM 2014*, 2014 Int. Conf. Optim. Electr. Electron. Equip. (2014) 713–720, https://doi.org/10.1109/OPTIM.2014.6850936.

[3] N.T.M. Balakrishnan, A. Das, N.S. Jishnu, L.R. Raphael, J.D. Joyner, J.H. Ahn, M. J. Jabeen Fatima, R. Prasanth, The great history of lithium-ion batteries and an overview on energy storage devices, Mater. Horiz. Nat. Nanomater. (2021) 1–21, https://doi.org/10.1007/978-981-15-8844-0_1.

[4] Y. Deng, Active electrode materials for high-performance lithium-ion battery, Highlights Sci. Eng. Technol. 121 (2024) 291–298, https://doi.org/10.54097/8A6EHB43.

[5] R. Pitchai, V. Thavasi, S.G. Mhaisalkar, S. Ramakrishna, Nanostructured cathode materials: a key for better performance in Li-ion batteries, J. Mater. Chem. 21 (30) (2011) 11040–11051, https://doi.org/10.1039/C1JM10857C.

[6] B.E. Murdock, K.E. Toghill, N. Tapia-Ruiz, A perspective on the sustainability of cathode materials used in lithium-ion batteries, Adv. Energy Mater. 11 (39) (2021) 2102028, https://doi.org/10.1002/AENM.202102028;REQUESTEDJOURNAL:JOURNAL:16146840;WGROUP:STRING:PUBLICATION.

[7] F. Soavi, A. Gregucci, A. Liverani, S. Mojtahedi, E. Petri, F. Mascetti, F. Capodarca, E. Bel Hadj Jrad, The European battery regulation and digital battery passport: prospects and challenges, **2026**, *12*, Batteries 12 (3) (2026), https://doi.org/10.3390/BATTERIES12030097.

[8] M. Wentker, M. Greenwood, M.C. Asaba, J. Leker, A Raw Material Criticality and Environmental Impact Assessment of State-of-the-Art and Post-Lithium-Ion Cathode Technologies, J. Energy Storage 26 (2019) 101022, https://doi.org/10.1016/J.EST.2019.101022.

[9] R. Deberdt, P. Le Billon, The Green Transition in Context—Cobalt Responsible Sourcing for Battery Manufacturing, Soc. Nat. Resour. 35 (7) (2022) 784–803, https://doi.org/10.1080/08941920.2022.2049410;REQUESTEDJOURNAL:JOURNAL:USNR20;WGROUP:STRING:PUBLICATION.

[10] Blair, J.J.A.; Balcázar, R.M.; Barandiarán, J.; Maxwell, A. The 'Alterlives' of Green Extractivism: Lithium Mining and Exhausted Ecologies in the Atacama Desert. http://journals.openedition.org/poldev 2023, No. 16. https://doi.org/10.4000/POLDEV.5284.

[11] G. Mishra, R. Jha, A. Meshram, K.K. Singh, A Review on Recycling of Lithium-Ion Batteries to Recover Critical Metals, J. Environ. Chem. Eng. 10 (6) (2022) 108534, https://doi.org/10.1016/J.JECE.2022.108534.
[12] T.T. Hailemariam, T.S. Birkneh, Advances in Sustainable Battery Technologies: Enhancing Longevity, Recycling, and Alternative Components– A Review, *2024, Volume 12, Page 77*, Am. J. Appl. Chem. 12 (4) (2024) 77–88, https://doi.org/10.11648/J.AJAC.20241204.11.
[13] V.M. Leal, J.S. Ribeiro, E.L.D. Coelho, M.B.J.G. Freitas, Recycling of Spent Lithium-Ion Batteries as a Sustainable Solution to Obtain Raw Materials for Different Applications, J. Energy Chem. 79 (2023) 118–134, https://doi.org/10.1016/J.JECHEM.2022.08.005.
[14] A. Mayyas, K. Moawad, A. Chadly, E. Alhseinat, Can Circular Economy and Cathode Chemistry Evolution Stabilize the Supply Chain of Li-Ion Batteries? Extr. Ind. Soc. 14 (2023) 101253 https://doi.org/10.1016/J.EXIS.2023.101253.
[15] P. Cattaneo, L. De Vita, C. Zanoni, D. Ruzza, M. Colantuono, D. Di Cintio, C. Cavallo, M. Copley, E. Quartarone, How Research & Innovation Ramp up Li-Ion Battery Recycling, J. Power Sources Adv. 37 (2026) 100198, https://doi.org/10.1016/j.powera.2025.100198.
[16] L. Gaines, J. Zhang, X. He, J. Bouchard, H.E. Melin, Tracking Flows of End-of-Life Battery Materials and Manufacturing Scrap, Batteries 9 (7) (2023) 360, https://doi.org/10.3390/BATTERIES9070360/S1.
[17] D. Marchese, C. Giosuè, A. Staffolani, M. Conti, S. Orcioni, F. Soavi, M. Cavalletti, P. Stipa, An Overview of the Sustainable Recycling Processes Used for Lithium-Ion Batteries, *2024, Vol. 10, Page 27*, Batteries 10 (1) (2024) 27, https://doi.org/10.3390/BATTERIES10010027.
[18] M.A. Rajaeifar, M. Raugei, B. Steubing, A. Hartwell, P.A. Anderson, O. Heidrich, Life Cycle Assessment of Lithium-Ion Battery Recycling Using Pyrometallurgical Technologies, J. Ind. Ecol. 25 (6) (2021) 1560–1571, https://doi.org/10.1111/JIEC.13157;WGROUP:STRING:PUBLICATION.
[19] E. Asadi Dalini, G. Karimi, S. Zandevakili, M. Goodarzi, A Review on Environmental, Economic and Hydrometallurgical Processes of Recycling Spent Lithium-Ion Batteries, Mineral. Process. Extr. Metall. Rev. (2020) 1–22, https://doi.org/10.1080/08827508.2020.1781628;JOURNAL:JOURNAL:GMPR20;REQUESTEDJOURNAL:JOURNAL:GMPR20;PAGE:STRING:ARTICLE/CHAPTER.
[20] J.J. Roy, D.M. Phuong, V. Verma, R. Chaudhary, M. Carboni, D. Meyer, B. Cao, M. Srinivasan, Direct Recycling of Li-Ion Batteries from Cell to Pack Level: Challenges and Prospects on Technology, Scalability, Sustainability, and Economics, Carbon Energy 6 (6) (2024) e492, https://doi.org/10.1002/CEY2.492;PAGEGROUP:STRING:PUBLICATION.
[21] Y. Sun, Lithium-Ion Battery Recycling: Challenges and Opportunities, Highlights Sci. Eng. Technol. 58 (2023) 365–370, https://doi.org/10.54097/HSET.V58I.10124.
[22] THE EUROPEAN PARLIAMENT AND THE COUNCIL OF THE EUROPEAN UNION. *Annex XVII to REACH (Regulation concerning the Registration, Evaluation, Authorisation and Restriction of Chemicals, Regulation - 1907/2006 - EN - REACH - EUR-Lex*. https://eur-lex.europa.eu/eli/reg/2006/1907/oj (accessed 2025-12-12).
[23] L. Oliveira, M. Messagie, S. Rangaraju, J. Sanfelix, M. Hernandez Rivas, J. Van Mierlo, Key Issues of Lithium-Ion Batteries – from Resource Depletion to Environmental Performance Indicators, J. Clean. Prod. 108 (2015) 354–362, https://doi.org/10.1016/J.JCLEPRO.2015.06.021.
[24] Y. He, X. Yuan, G. Zhang, H. Wang, T. Zhang, W. Xie, L. Li, A Critical Review of Current Technologies for the Liberation of Electrode Materials from Foils in the Recycling Process of Spent Lithium-Ion Batteries, Sci. Total. Environ. 766 (2021), https://doi.org/10.1016/j.scitotenv.2020.142382.
[25] D. Pant, T. Dolker, Green and Facile Method for the Recovery of Spent Lithium Nickel Manganese Cobalt Oxide (NMC) Based Lithium Ion Batteries, Waste Manag. 60 (2017) 689–695, https://doi.org/10.1016/J.WASMAN.2016.09.039.
[26] Y. Bai, W.B. Hawley, C.J. Jafta, N. Muralidharan, B.J. Polzin, I. Belharouak, Sustainable Recycling of Cathode Scraps via Cyrene-Based Separation, Sustain. Mater. Technol. 25 (2020) e00202, https://doi.org/10.1016/J.SUSMAT.2020.E00202.
[27] A. Staffolani, F. Mascetti, A. Trebbi, A. Gregucci, S. Mojtahedi, F. Soavi, Sustainable and Direct Recovery of Lithium-Ion Battery Cathodes From Production Scraps, ChemElectroChem 13 (9) (2026) e202500470, https://doi.org/10.1002/CELC.202500470.
[28] Y. Yao, M. Zhu, Z. Zhao, B. Tong, Y. Fan, Z. Hua, Hydrometallurgical Processes for Recycling Spent Lithium-Ion Batteries: A Critical Review, ACS Sustain. Chem. Eng. 6 (11) (2018) 13611–13627, https://doi.org/10.1021/ACSSUSCHEMENG.8B03545.
[29] W. hao Gao, C. chen Nie, L. Li, S. Yan, W. tao Zhou, X. nan Zhu, Sustainable and Efficient Deep Eutectic Solvents in Recycling of Spent Lithium-Ion Batteries: Recent Advances and Perspectives, J. Clean. Prod. 464 (2024) 142735, https://doi.org/10.1016/J.JCLEPRO.2024.142735.
[30] C. Zanoni, D. Callegari, D. Merli, P. Mustarelli, E. Quartarone, A Solvometallurgical Approach for the Recovery of Valuable Metals in the Recycling of End-of-Life Batteries, J. Power Sources 662 (39) (2026) 238795, https://doi.org/10.1016/j.jpowsour.2025.238795.
[31] M. Shaibuna, L.V. Theresa, K. Sreekumar, Neoteric Deep Eutectic Solvents: History, Recent Developments, and Catalytic Applications, Soft Matter 18 (14) (2022) 2695–2721, https://doi.org/10.1039/D1SM01797G.
[32] K.A. Omar, R. Sadeghi, Database of Deep Eutectic Solvents and Their Physical Properties: A Review, J. Mol. Liq. 384 (2023) 121899, https://doi.org/10.1016/J.MOLLIQ.2023.121899.
[33] B.K. Chakrabarti, M. Hayyan, S.S. Syed Putra, T.Y. İnan, T. Mu, L.S. Zulkifli, N.S. A. Manan, W.J. Basirun, Y. Qiao, M.K. Bayazıt, S. Hayat Soytaş, J. Rubio-Garcia, N. Shah, I.M. AlNashef, J.P. Hallett, Y.S. Hajimolana, C.T.J. Low, Deep Eutectic Solvents in Battery Recycling: A Sustainable Path Forward, J. Power Sources 670 (2026) 239475, https://doi.org/10.1016/J.JPOWSOUR.2026.239475.
[34] S. Zheng, S. Xu, Z. Wang, H. Duan, D. Chen, M. Long, Y. Li, Efficient Leaching of Valuable Metals from Spent Lithium-Ion Batteries Using Green Deep Eutectic Solvents: Process Optimization, Mechanistic Analysis, and Environmental Impact Assessment, J. Clean. Prod. 480 (2024) 144128, https://doi.org/10.1016/J.JCLEPRO.2024.144128.
[35] S. Liu, S. Li, X.E. Cao, S. Choi, An Ultra-Fast and Eco-Friendly Recycling Process for Spent LIBs Using Deep Eutectic Solvents: Mechanism and Life-Cycle Insight, Green. Chem. 27 (45) (2025) 14648–14657, https://doi.org/10.1039/D5GC03452C.
[36] B. Li, Q. Li, Q. Wang, X. Yan, M. Shi, C. Wu, Deep Eutectic Solvent for Spent Lithium-Ion Battery Recycling: Comparison with Inorganic Acid Leaching, Phys. Chem. Chem. Phys. 24 (32) (2022) 19029–19051, https://doi.org/10.1039/D1CP05968H.
[37] K. Kurniawan, S. Kim, M. Bae, J. chun Lee, A. Chagnes, Non-Aqueous Leaching of Critical Metals from Black Mass of Spent Lithium-Ion Batteries Using a Reusable Acidic Organophosphorus Extractant, J. Environ. Manag. 397 (2026) 128220, https://doi.org/10.1016/J.JENVMAN.2025.128220.
[38] F. Sitorus, E. Stromberg, L. Rouquette, K. André, K.A.N. Vorland, M. Khalifeh, D. Wragg, M. Petranikova, D. Yilmaz, Sustainable Leaching of Critical Metals from Lithium Ion Battery Black Mass Using a Citric Acid and Choline Chloride Deep Eutectic Solvent, *2025 6:1*, Discov. Sustain. 6 (1) (2025) 1298, https://doi.org/10.1007/S43621-025-02214-5.
[39] F. Nazlı, I. Hasdemir, E. Uysal, H.N. Dursun, U.O. Gezici, D.Y. Özçelik, F. Burat, S. Gürmen, Eco-Friendly Leaching of Spent Lithium-Ion Battery Black Mass Using a Ternary Deep Eutectic Solvent System Based on Choline Chloride, Glycolic Acid, and Ascorbic Acid, *2025, Vol. 15*, Minerals 15 (8) (2025), https://doi.org/10.3390/MIN15080782.
[40] W. Ma, M. Liu, X. Zhang, Q. Zhao, Z. Liang, An Efficient and Precipitant-Free Approach to Selectively Recover Lithium Cobalt Oxide Made for Cathode Materials Using a Microwave-Assisted Deep Eutectic Solvent, Energy & Fuels 37 (1) (2022) 724–734, https://doi.org/10.1021/ACS.ENERGYFUELS.2C03242.
[41] N. Rodriguez Rodriguez, A. Van Den Bruinhorst, L.J.B.M. Kollau, M.C. Kroon, K. Binnemans, Degradation of Deep-Eutectic Solvents Based on Choline Chloride and Carboxylic Acids, ACS Sustain. Chem. Eng. 7 (13) (2019) 11521–11528, https://doi.org/10.1021/ACSSUSCHEMENG.9B01378.
[42] D. Pradhan, S. Jaiswal, B.K. Tiwari, A.K. Jaiswal, Choline Chloride – Oxalic Acid Dihydrate Deep Eutectic Solvent Pretreatment of Barley Straw for Production of Cellulose Nanofibers, Int. J. Biol. Macromol. 281 (2024) 136213, https://doi.org/10.1016/J.IJBIOMAC.2024.136213.
[43] Y. Yu, D. Wang, L. Chen, H. Qi, A. Liu, M. Deng, X. Wu, K. Wang, Recyclable Choline Chloride-Based Deep Eutectic Solvent Pretreatment for Accelerated Enzymatic Digestibility of Triarrhena Lutarioriparia, Ind. Crops Prod. 187 (2022) 115542, https://doi.org/10.1016/J.INDCROP.2022.115542.
[44] ISO 14044:*2006 - Environmental management — Life cycle assessment — Requirements and guidelines.* https://www.iso.org/standard/38498.html (accessed 2026-02-25).
[45] ISO 14040:*2006 - Environmental management — Life cycle assessment — Principles and framework.* https://www.iso.org/standard/37456.html (accessed 2026-02-19).
[46] R. Arvidsson, M. Svanström, B.A. Sandén, N. Thonemann, B. Steubing, S. Cucurachi, Terminology for Future-Oriented Life Cycle Assessment: Review and Recommendations, *2023 29:4*, Int. J. Life Cycle Assess. 29 (4) (2023) 607–613, https://doi.org/10.1007/s11367-023-02265-8.
[47] T. Ekvall, G. Assefa, A. Björklund, O. Eriksson, G. Finnveden, What Life-Cycle Assessment Does and Does Not Do in Assessments of Waste Management, Waste Manag. 27 (8) (2007) 989–996, https://doi.org/10.1016/J.WASMAN.2007.02.015.
[48] M.Z. Hauschild, R.K. Rosenbaum, S.I. Olsen, Life Cycle Assessment: Theory and Practice, Life Cycle Assess. Theory Pract. (2017) 1–1216, https://doi.org/10.1007/978-3-319-56475-3/SAVE-RESEARCH.
[49] ecoinvent v3.11 - ecoinvent https://ecoinvent.org/ecoinvent-v3-11/ (accessed 2026-06-08).
[50] *Procedural life cycle inventory of chemical products at laboratory and pilot scale: a compendium - Green Chemistry (RSC Publishing)* DOI:10.1039/D4GC01372G. https://pubs.rsc.org/en/content/articlehtml/2024/gc/d4gc01372g (accessed 2026-06-08).
[51] B.P. Weidema, M.S. Wesnæs, Data Quality Management for Life Cycle Inventories-an Example of Using Data Quality Indicators, J. Clean. Prod. 4 (3–4) (1996) 167–174, https://doi.org/10.1016/S0959-6526(96)00043-1.
[52] E. Rossi, D. Cespi, I. Maggiore, L. Setti, F. Passarini, Energy from Waste Biomass: An LCA Study on a Biofuel Cell at Early Design Stage, Environ. Sci. Pollut. Res. 2024 (2024) 1–16, https://doi.org/10.1007/s11356-024-34068-1.
[53] F. Piccinno, R. Hischier, S. Seeger, C. Som, From Laboratory to Industrial Scale: A Scale-up Framework for Chemical Processes in Life Cycle Assessment Studies, J. Clean. Prod. 135 (2) (2016) 1085–1097, https://doi.org/10.1016/j.jclepro.2016.06.164.
[54] Pan Xiaoming; Qiu Guocai; Li Guangping. Preparation Method of Triethyl Phosphate - CN103374028A, October 30, 2013. https://patents.google.com/patent/CN103374028A/en (accessed 2026-03-10).
[55] Xu Yongjiang; Wang Qin; Jiang Wenyu; Yue Lizhen; Fang Ling; Ding Xianhua The Manufacture Method of Choline Chloride 60 - CN1078231A, November 10, 1993. https://patents.google.com/patent/CN1078231A/en (accessed 2026-03-10).
[56] IDEA – Inventory Database for Environmental Analysis. https://idea-lca.com/en/ (accessed 2026-06-08).

[57] R. Hischier, S. Hellweg, C. Capello, A. Primas, Establishing Life Cycle Inventories of Chemicals Based on Differing Data Availability, Int. J. Life Cycle Assess. 10 (1) (2005) 59–67, https://doi.org/10.1065/LCA2004.10.181.7/METRICS.
[58] M.A.J. Huijbregts, Z.J.N. Steinmann, P.M.F. Elshout, G. Stam, F. Verones, M. Vieira, M. Zijp, A. Hollander, R. van Zelm, ReCiPe2016: A Harmonised Life Cycle Impact Assessment Method at Midpoint and Endpoint Level, *2016 22:2*, Int. J. Life Cycle Assess. 22 (2) (2016) 138–147, https://doi.org/10.1007/s11367-016-1246-y.
[59] B. Jaleh, N. Gavar, P. Fakhri, N. Muensit, S.M. Taheri, Characteristics of PVDF Membranes Irradiated by Electron Beam, *2015, Vol. 5, Pages 1-10*, Membranes 5 (1) (2015) 1–10, https://doi.org/10.3390/MEMBRANES5010001.
[60] A.T.S. Freiberg, J. Sicklinger, S. Solchenbach, H.A. Gasteiger, Li2CO3 Decomposition in Li-Ion Batteries Induced by the Electrochemical Oxidation of the Electrolyte and of Electrolyte Impurities, Electrochim. Acta 346 (2020) 136271, https://doi.org/10.1016/J.ELECTACTA.2020.136271.
[61] M. Svärd, C. Ma, K. Forsberg, P.G. Schiavi, Addressing the Reuse of Deep Eutectic Solvents in Li-Ion Battery Recycling: Insights into Dissolution Mechanism, Metal Recovery, Regeneration and Decomposition, ChemSusChem 17 (20) (2024) e202400410, https://doi.org/10.1002/CSSC.202400410;JOURNAL:JOURNAL:1864564X;PAGEGROUP:STRING:PUBLICATION.
[62] N. Peeters, K. Binnemans, S. Riaño, Solvometallurgical Recovery of Cobalt from Lithium-Ion Battery Cathode Materials Using Deep-Eutectic Solvents, Green. Chem. 22 (13) (2020) 4210–4221, https://doi.org/10.1039/D0GC00940G.
[63] C.W. Tang, C.Bin Wang, S.H. Chien, Characterization of Cobalt Oxides Studied by FT-IR, Raman, TPR and TG-MS, Thermochim. Acta 473 (1–2) (2008) 68–73, https://doi.org/10.1016/J.TCA.2008.04.015.
[64] M. Aadil, S. Zulfiqar, M.F. Warsi, P.O. Agboola, I. Shakir, Free-Standing Urchin-like Nanoarchitectures of Co3O4 for Advanced Energy Storage Applications, J. Mater. Res. Technol. 9 (6) (2020) 12697–12706, https://doi.org/10.1016/j.jmrt.2020.08.110.
[65] Z.P. Xu, H.C. Zeng, Thermal Evolution of Cobalt Hydroxides: A Comparative Study of Their Various Structural Phases, J. Mater. Chem. 8 (11) (1998) 2499–2506, https://doi.org/10.1039/a804767g.
[66] S. Moon, W. Chae, B.M. Jun, Y. Yoon, H. Rho, Comparative Study on the Leaching Behavior of Lithium-Ion Battery Black Mass Using Sulfuric and Organic Acids Combined with Hydrogen Peroxide, Sep. Purif. Technol. 376 (2025) 133991, https://doi.org/10.1016/J.SEPPUR.2025.133991.
[67] F. Wang, R. Sun, J. Xu, Z. Chen, M. Kang, Recovery of Cobalt from Spent Lithium Ion Batteries Using Sulphuric Acid Leaching Followed by Solid–Liquid Separation and Solvent Extraction, RSC Adv. 6 (88) (2016) 85303–85311, https://doi.org/10.1039/C6RA16801A.
[68] M. Shahid, S.A. Sahadevan, V. Ramani, S. Sankarasubramanian, Recommended Practices for the Electrochemical Recovery of Cobalt from Lithium Cobalt Oxide: A Case Study of the Choline Chloride:Ethylene Glycol Deep Eutectic Solvent, ChemSusChem 18 (3) (2025) e202401205, https://doi.org/10.1002/CSSC.202401205.
[69] X. Li, Y. Li, Q. Qiao, K. Wang, H. Yu, Recovery of Cobalt from Cathode of Lithium-Ion Battery Using Ternary Deep Eutectic Solvent, *2024 41:12*, Korean J. Chem. Eng. 41 (12) (2024) 3151–3161, https://doi.org/10.1007/S11814-024-00253-8.
[70] C. Wang, T. Ai, X. Gao, J. Lu, J. Liu, W. Zhu, Y. Luo, Effective Recycling of Critical Metals from LiCoO2 Batteries by Hydrated Deep Eutectic Solvents: Performance, Kinetic and Mechanism, J. Water Process. Eng. 59 (2024) 105088, https://doi.org/10.1016/J.JWPE.2024.105088.
[71] S. Tang, M. Zhang, M. Guo, A Novel Deep-Eutectic Solvent with Strong Coordination Ability and Low Viscosity for Efficient Extraction of Valuable Metals from Spent Lithium-Ion Batteries, ACS Sustain. Chem. Eng. 10 (2) (2022) 975–985, https://doi.org/10.1021/ACSSUSCHEMENG.1C06902.
[72] R. Heijungs, Probability, Statistics and Life Cycle Assessment: Guidance for Dealing with Uncertainty and Sensitivity. *Probability*, Stat. Life Cycle Assess. Guid. Deal. Uncertain. Sensit. (2024) 1–1158, https://doi.org/10.1007/978-3-031-49317-1/SAVE-RESEARCH.
[73] A.Y. Hoekstra, M.M. Mekonnen, The Water Footprint of Humanity, Proc. Natl. Acad. Sci. U. S. A. 109 (9) (2012) 3232–3237, https://doi.org/10.1073/pnas.1109936109.
[74] G. Pallas, M.G. Vijver, W.J.G.M. Peijnenburg, J. Guinée, Life cycle assessment of emerging technologies at the lab scale: the case of nanowire-based solar cells, J. Ind. Ecol. 24 (1) (2020) 193–204, https://doi.org/10.1111/JIEC.12855;WEBSITE:WEBSITE:PERICLES;REQUESTEDJOURNAL:JOURNAL:15309290;WGROUP:STRING:PUBLICATION.
[75] H. Li, N. Chen, W. Liu, H. Feng, J. Su, D. Fu, X. Liu, M. Qiu, L. Wang, A Reusable Deep Eutectic Solvent for the Regeneration of Li and Co Metals from Spent Lithium-Ion Batteries, J. Alloy. Compd. 966 (2023) 171517, https://doi.org/10.1016/J.JALLCOM.2023.171517.
[76] K. Binnemans, P.T. Jones, Ionic liquids and deep-eutectic solvents in extractive metallurgy: mismatch between academic research and industrial applicability, *2023 9:2*, J. Sustain. Metall. 9 (2) (2023) 423–438, https://doi.org/10.1007/S40831-023-00681-6.
[77] M.K. Tran, M.T.F. Rodrigues, K. Kato, G. Babu, P.M. Ajayan, Deep eutectic solvents for cathode recycling of Li-Ion batteries, *2019 4:4*, Nat. Energy 4 (4) (2019) 339–345, https://doi.org/10.1038/s41560-019-0368-4.
[78] A.-M. Popescu, C. Donath, V. Constantin, Density, Viscosity and Electrical Conductivity of Three Choline Chloride Based Ionic Liquids, Bulg. Chem. Commun. 46 (3) (2014) 452–457.
[79] J. Naser, F.S. Mjalli, Z.S. Gano, Molar Heat Capacity of Selected Type III Deep Eutectic Solvents, J. Chem. Eng. Data 61 (4) (2016) 1608–1615, https://doi.org/10.1021/ACS.JCED.5B00989.
[80] A. Kityk, V. Pavlik, M. Hnatko, Reshaping the Future of Battery Waste: Deep Eutectic Solvents in Li-Ion Battery Recycling, J. Energy Storage 97 (2) (2024) 112990, https://doi.org/10.1016/j.est.2024.112990.
[81] J. Dewulf, L. Benini, L. Mancini, S. Sala, G.A. Blengini, F. Ardente, M. Recchioni, J. Maes, R. Pant, D. Pennington, Rethinking the Area of Protection "Natural Resources" in Life Cycle Assessment, Environ. Sci. Technol. 49 (9) (2015) 5310–5317, https://doi.org/10.1021/acs.est.5b00734.
[82] Study on the critical raw materials for the EU 2023 - Publications Office of the EU. https://op.europa.eu/en/publication-detail/-/publication/57318397-fdd4-11ed-a05c-01aa75ed71a1/language-en (accessed 2026-03-10).
[83] I. Hackenhaar, R.A.F. Alvarenga, T.M. Bachmann, F. Riva, R. Horn, R. Graf, J. Dewulf, A critical review of criticality methods for a european life cycle sustainability assessment, Procedia CIRP 105 (2022) 428–433, https://doi.org/10.1016/j.procir.2022.02.071.